ACS APPLIED MATERIALS & INTERFACES

Research Article

www.acsami.org

Synthesis and Bidirectional Frequency Tuning of Cantilever-Shape Nano Resonators Using a Focused Ion Beam

Jiyoung Chang,[†] Kisik Koh,[‡] Byung-Kwon Min,[§] Sang Jo Lee,[§] Jongbaeg Kim,*[,§] and Liwei Lin[‡]

[†]Center of Integrated Nanomechanical Systems, University of California at Berkeley, Berkeley, California, 94720 United States

[‡]Berkeley Sensor and Actuator Center, Department of Mechanical Engineering, University of California at Berkeley, Berkeley, California, 94720 United States

[§]School of Mechanical Engineering, Yonsei University, Seoul, 120-749 South Korea

ABSTRACT: The synthesis of cantilever-shape nano resonators and their resonant frequency tunings in both upward and downward directions have been demonstrated using FIB-CVD (focused ion beam-chemical vapor deposition). The in situ experimental observations of mechanical resonances as well as cutting and adding of resonator materials have been accomplished inside the FIB vacuum chamber. Extending the length of the cantilever-shape resonator by 500 nm scale using either the same material or alternating different materials effectively reduced resonant frequency. On the other hand, direct cutting and gradual trimming of the end point of nano resonator increases its resonant frequency. This simple yet versatile synthesis and frequency tuning scheme could be applicable to both constructing micro/nano scale resonators and tuning nanostructures with reduced efforts and enhanced efficiency.

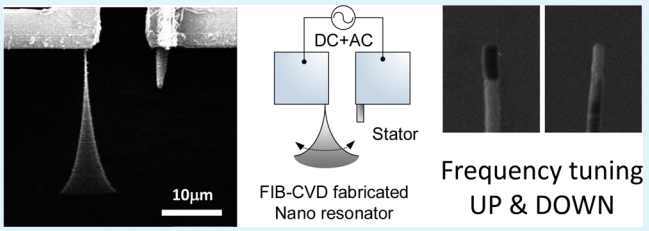

KEYWORDS: *frequency tuning, nano resonator, focused ion beam CVD, bidirectional frequency tuning*

1. INTRODUCTION

Micro/nano scale devices that utilize mechanical resonance have been proposed for applications in various high precision sensors,[1] including gyroscopes,[2] and communication systems such as mechanical filters.[3] These micro- and nanomachined structures inevitably have dimensional errors due to tolerance in the machining processes. As a result, frequency matching of mechanical resonance is often required after the completion of the fabrication process. There are several prior studies dealing with resonant frequency tuning of micro and nano resonators utilizing either active or passive methods. The methodology of active frequency tuning requires continuous power supply to temporarily alter the stiffness or the stress of the mechanical resonators. Prior works include the utilization of the electrostatic spring softening effect,[4] the usage of a seismic mass to affect the total stiffness,[5] the application of an adaptive frequency tuning scheme,[2] various comb structure profiles,[6] and the adoption of thermal expansion[7] or local thermal stress effects.[8] The passive tuning method, on the other hand, either adds or removes materials from the mechanical resonators to change the effective mass or stiffness of the resonators. Notable works include the mass alteration by pulsed laser deposition,[9] selective polysilicon deposition using a local chemical vapor deposition (CVD) process,[10] electrochemical deposition,[11] localized deposition and annealing,[12] and the application of a mass migration process on a cantilevered MWCNT (multi wall carbon nanotube) nano resonator.[13] The majority of these previous demonstrations of active or passive frequency tunings on micro or nano resonators are one-directional. In other words, these schemes either increase or reduce the resonant frequencies of fabricated resonators.

A focused ion beam (FIB) has been used to fabricate micro- and nanostructures with the capability of controllable sputtering and deposition processes at sub-micrometer resolution. For example, researchers have demonstrated the three dimensional micro- and nanostructures, such as 3D tools[14] and rotors.[15] In the microelectromechanical systems (MEMS) field, a FIB has been used in a passive frequency tuning scheme by alternating the stiffness of a micro resonator.[16] However, the process was only able to lower the resonant frequency. Other FIB tuning demonstrations utilized the mass addition procedure[17] for ultrasensitive mass sensors,[18] and the active frequency tuning of a beam shaped nano resonator was demonstrated under continuous activation of a counter electrode. Although the procedure is highly effective, it requires unceasing power supply to maintain the frequency tuning status.

In this work, single and multi-step frequency tuning processes were developed using the FIB-CVD. The frequency tuning and frequency monitoring processes were conducted in situ without removing the specimen from the vacuum chamber. The capability of conducting permanent and precise frequency tuning in an efficient manner as demonstrated in this paper can pave the wave for interesting applications based on micro/nano

Received: July 9, 2013
Accepted: September 11, 2013
Published: September 11, 2013

   dx.doi.org/10.1021/am402738g | *ACS Appl. Mater. Interfaces* 2013, 5, 9684−9690

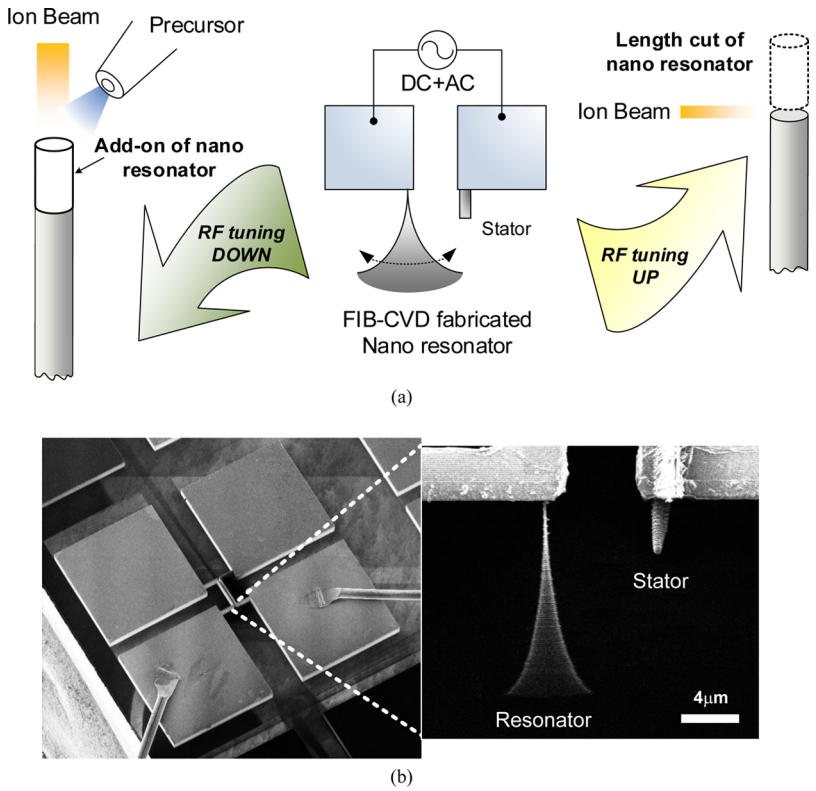

Figure 1. Schematic diagram of the synthesis and bidirectional frequency tuning of cantilever-shape nano resonators using FIB-CVD. (a) Nano resonator is driven electrostatically to its resonant frequency. The FIB deposition process (left) and sputtering process (right) can be used to add and remove materials from the nano resonator to reduce and increase its resonant frequencies. The whole procedure including the fabrication, operation, and frequency tuning can be performed inside the FIB vacuum chamber. (b) Scanning ion microscope (SIM) image of the silicon chip with wire bonds (left). The nano resonators are synthesized on top of the micromachined structures. Cantilever-shape resonators are constructed on top of the micromachined structures. The nano resonator and the stator are electrically separated by a 5 μm wide gap and positioned at the edge of micro electrodes. Exposure time was adjusted to capture nano resonator in resonance in which a triangular shape is recorded (right). Nano resonator vibrates in the lateral direction when the applied actuation frequency matches its own resonant frequency.

mechanical resonators where frequency matching is critical for enhanced performance.

2. EXPERIMENTAL SECTION

2.1. Design and Fabrication of Carbon- and Tungsten-Based Nano Resonators. Figure 1a illustrates the overall scheme of the synthesis and bidirectional tuning of cantilever-shape nano resonators. The cantilever-shape nano resonator and the actuation stator are constructed using either carbon- or tungsten-based FIB-CVD. The resonant frequency was passively adjusted either by adding materials to extend the total length of the resonator using the FIB deposition process or by removing materials to reduce the entire length via the FIB sputtering process. The stator, which works as the stationary counter electrode, 1 μm in diameter and 5 μm in length, was designed to be shorter and much stiffer than the cantilever-shape resonator whose dimension ranges as 150 nm in diameter and up to 15 μm in length. The SIM (scanning ion microscopy) image in Figure 1b shows a MEMS (microelectromechanical systems) structure on which the resonator and the stator were located. The close-up SIM image on the right side clearly illustrates nano resonator under resonance and a stationary stator. Triangular shape when the image is captured is attributed to faster resonance frequency of nano resonator than SIM scanning frequency. The MEMS platform was fabricated using a single-mask, SOI (silicon-on-insulator) process.[19] The starting material was a heavily doped SOI wafer such that the silicon device layer can be considered as a good conductor. The DRIE (deep reactive ion etching) process was used to define the MEMS electrodes which are electrically isolated with each other by the 5 μm-wide gaps. The contact electrodes are connected to a dual in-line package via the wire bonding that serves as electrical input connectors to the outside function generator. Electrostatic force was induced via the combination of both DC and AC voltage inputs. When the input frequency of the AC input approaches the resonant frequency of the nano resonator, the resonator started vibration laterally.

The 13 nm in diameter Ga^+ beam was used in the FIB-CVD process (focused ion beam machine SII3050 from SEIKO Instruments Incorporation) with continuously supplied precursors of phenanthrene vapor ($C_{14}H_{10}$) for carbon-based deposition and tungsten hexacarbonyl ($W(CO)_6$) for tungsten-based deposition. Previous works related to the FIB-CVD process estimated Young's modulus of carbon-based[20] and tungsten-based depositions[21] to be 80−300 GPa and 200−300 GPa and density to be 2300−4000 and 1300 kg/m^3, respectively. Specifically, our previous work on FIB-CVD estimated the Young's modulus of carbon-based material to be 84.5 GPa[22] based on the analysis of nano tweezers operation. During the synthesis process, the ion irradiation time was adjusted to control the length of the deposited nanostructures while the diameter of the structure is controlled by adjusting the beam current. In this study, nano resonators with diameter of 150 nm have been fabricated by using the beam current of 9.1pA. At given condition, it took about 10 minutes to fabricate a carbon-based nano resonator of 8 μm in length and 150 nm in diameter with a deposition rate of 0.05 μm^3/min, whereas it took 15 minutes to fabricate a tungsten-based nano resonator of 8 μm in length and 150 nm in diameter with a deposition rate of 0.03 μm^3/min. A relatively long processing time to make a single resonator is related to smooth cylindrical shape. Faster deposition rate is able to create pillar structure as well; however, the final product easily ends up with bumpy surface which is believed to be due to not enough ion beam irradiation. In addition to that, the FIB-CVD utilizes a single column and the overall productivity is not high

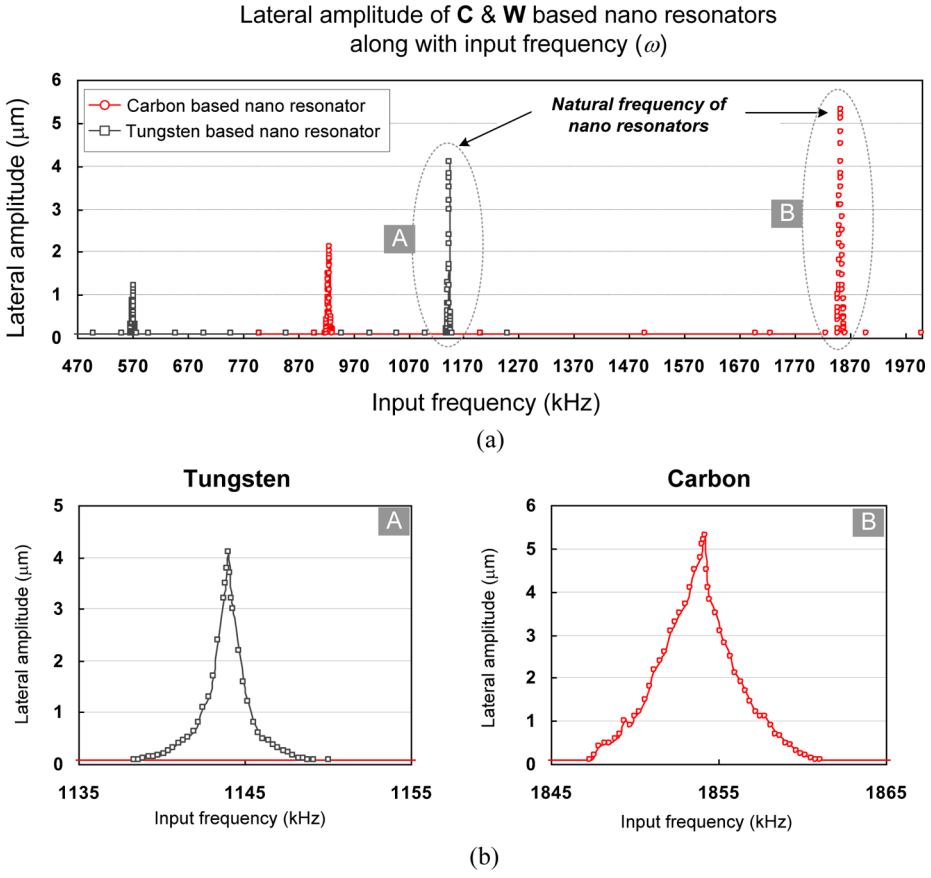

Figure 2. (a) Tip vibration displacements of carbon and tungsten nano resonators versus applied frequencies. The applied DC and AC voltages result in two resonance peaks at frequency ω and 2ω. (b) Frequency responses for tungsten-based (left) and carbon-based (right) nano resonators and Q-factor is estimated to be 100 and 300, respectively.

which could be resolved via building a multi-columns set-up in the future.

2.2. Frequency Responses of Nano Resonators. Experimentally, a 5-volt AC input on top of a 5-volt DC bias was applied to the nano resonator inside the FIB chamber via the electrical contact pads in the chamber kept at $6.3 \pm 0.2 \times 10^5$ Pa. The lowest available dose/resolution scanning was used to prevent possible measurement errors caused by continuous ion beam irradiation to the nano resonators. Specifically, strong ion beam exposure could cause the implantation of gallium ions and change their morphological shape and property.[23] The amplitude of lateral movement captured in resonance was recorded with corresponding frequency to evaluate the mechanical resonance and Q-factor of nano resonators. This inevitably brought limitation in measurement accuracy. As the resonance detection solely depends on visual monitoring, the lowest possible ion beam irradiation and shortest exposure time was used, by which the measured resonance has 3 significant figures of accuracy. Improving measurement accuracy to 5 significant figures is underway using capacitance measurement with counter electrodes.

Figure 2 plots the amplitude of the lateral movement of an 8.6 μm-long carbon and an 8.3 μm-long tungsten-based nano resonator with respect to the actuating frequency from 470 to 1570 kHz. The first resonant frequency of the carbon-based nano resonator was observed at 927.1 kHz with a tip-displacement of 2.1 μm, and the second peak is detected at 1.8542 MHz with a tip-displacement of 5.3 μm. For the tungsten nano resonator, the first resonant frequency was recorded at 572 kHz with 1.2 μm tip-displacement and 1.144 MHz with 4.1 μm tip-displacement. Analytically, the voltage input applied contains both DC and AC components

$$V_{\text{input}} = V_{\text{DC}} + V_{\text{AC}}\sin(\omega t) \tag{1}$$

where ω is the applied frequency. The electrostatic force with input voltage V_{input} is expressed in terms of capacitance change

$$F_{\text{electrostatic}} = \frac{1}{2}\frac{\partial C}{\partial x}(V_{\text{input}})^2 \tag{2}$$

By using eqs 1 and 2, the electrostatic force was derived as follows

$$F_{\text{electrostatic}} = \frac{1}{2}\frac{\partial C}{\partial x}\left[{V_{\text{DC}}}^2 + \frac{1}{2}V_{\text{DC}}V_{\text{AC}}\sin(\omega t) - \frac{1}{2}{V_{\text{AC}}}^2\cos(2\omega t)\right] \tag{3}$$

As shown in eq 3, two frequency components, ω and 2ω are generated as the actuation force. It is noted that the natural frequency is the input frequency from the second peak since the first peak is excited by the 2ω component of the input. This phenomenon was observed experimentally as the first two resonant frequencies in each of the nano resonators have the exact ω and 2ω relationship. Furthermore, the excitation force from the 2ω effect is smaller (a minus term in eq 3) when compared to the ω effect (a plus term in eq 3). As a result, the observed displacement at the first resonant frequency was less than the displacement at the second resonant frequency in both nano resonators.

The resonant frequency of a cylindrical shaped beam can be derived as[24]

$$f_n = \frac{{\beta_n}^2}{2\pi \cdot L^2}\sqrt{\frac{E \cdot I}{\rho \cdot A}} \tag{4}$$

where L, ρ, A, and I are the length, density, cross section area, and moment of inertia of the nano resonator while β_n is a constant determined by the resonance mode (at the fundamental mode, β_0 = 1.875). Since our prototype nano resonators have similar geometry, Young's modulus and density are the dominant factors determining

the resonant frequency. The tungsten-based resonator is reported to show three to five times higher density (Table 1) and one to four times higher Young's modulus than the carbon-based resonator. When considering larger variation in density, the tungsten-based nano resonator is expected to have lower resonant frequency than the carbon-based nano resonator. The quality factors (Q-factors) of carbon- and tungsten-based nano resonator were estimated to be 100 and 300, respectively, on the basis of the response shown in Figure 2b,c. Such a low Q-factor than that of previously reported nano resonators[25] indicates possible larger internal energy losses. Nevertheless, after 30 minute operations at the resonance for both nano resonators, no visual degradation was detected and the resonant frequency did not change. The vacuum packaging and sealing is one of the important prerequisites in nano resonator operation. As there is no perfect hermetic sealing available yet, leakage is inevitable and corresponding performance degradation over time is expected as well. However, up to date vacuum packaging is widely adopted in commercialized devices such as the gyroscope, and reliable vacuum packaging is expected to minimize the resonance shift.

Table 1. Resonator Fabrication Condition in the FIB-CVD Process[23,24]

nano resonator fabrication condition		
	precursor materials	
parameters	phenanthrene vapor (C14H10)	tungsten hexacarbonyl (W(CO)6)
beam current (pA)	9.1	9.1
beam diameter (nm)	13	13
spot irradiation deposition rate (mm/min)	≈1	≈0.2
Young's modulus of deposited materials (GPa)	80−400	≈300
density (kg/m^3)	2300−4000	≈13 000
deposition rate (mm^3/min)	0.05	0.03

2.3. FIB-Based Frequency Tuning of Nano Resonators. The focused ion beam is capable of providing accurate local etching/deposition as well as good position control via ion beams and CVD for the frequency tuning of nano resonator. Figure 3 illustrates the possible tuning schemes. First, frequency reduction can be achieved by adding more length on top of preprocessed nano resonators. In this case, deposition location and ion dosage is precisely controlled to maintain the cylindrical shape of nano resonators (Figure 3a). Second, direct ion beam irradiation for discrete and coarse tuning can be applied to the tip region of the nano resonator for the purpose of tuning up (Figure 3b). With the nature of the Gaussian profile of the ion beam, it is difficult to cut small segments of nano resonator with good repeatability, so we set the minimum cutting length as 1 μm in the prototype demonstrations. After the direct cut, the small portion of the nano resonator can also be trimmed gradually via a longitudinal direction at the tip region as shown in Figure 3b, bottom right. The fine frequency increment of the nano resonator as small as a few kilohertz was achieved.

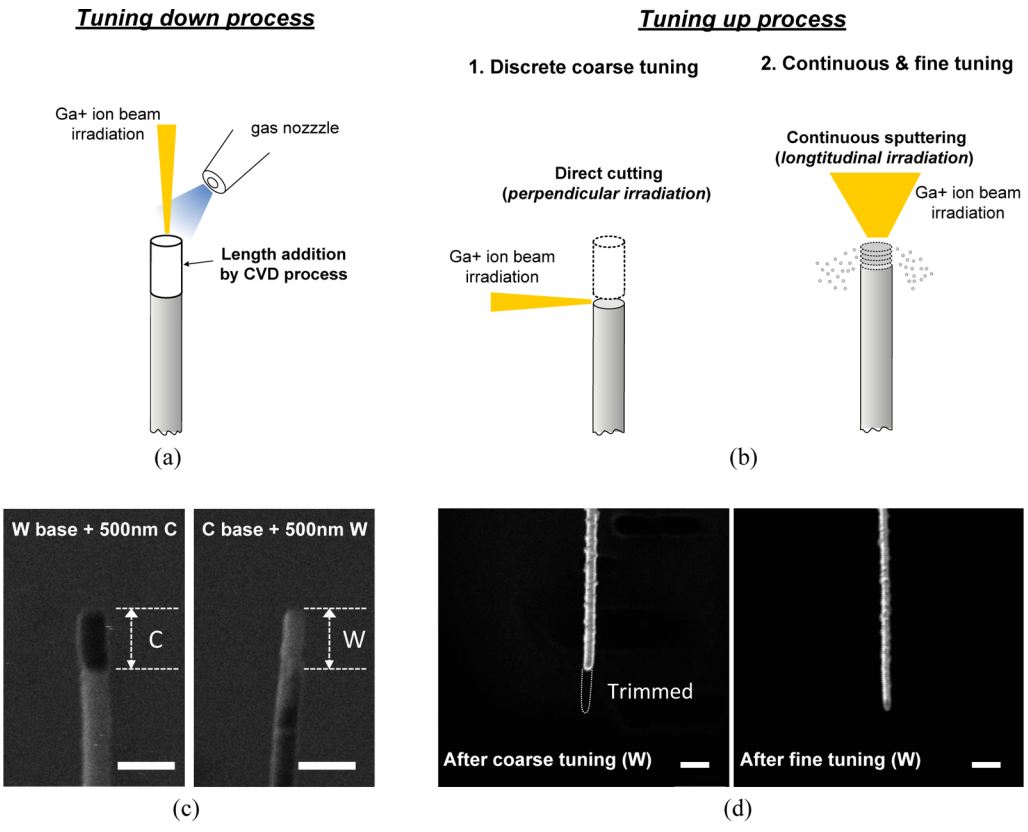

Figure 3. Frequency tuning processes for nano resonators. (a) Frequency reduction of the nano resonator is achieved by adding additional length at the tips of cantilever-shape nano resonators. (b) Coarse (direct) cutting with FIB in the directional perpendicular to the nano resonators and fine (continuous) sputtering with FIB in the direction parallel to the nano resonators are used to reduce the lengths of the nano resonators to increase their resonant frequencies. (c) The different contrast ratio in the SIM image indicates the difference of charge accumulation between carbon and tungsten segments. Scale bar: 500 nm. (d) SIM images at the end parts of two tungsten-based nano resonators after the coarse cutting (left) and continuous fine cutting (right) of the nano resonators. The sharpened end shape at the tip of the nano resonator after the fine tuning process is observed. There is no noticeable change of the cylindrical shape for both cases. Scale bar : 1 μm.

dx.doi.org/10.1021/am402738g | ACS Appl. Mater. Interfaces 2013, 5, 9684−9690

3. RESULTS AND DISCUSSION

3.1. Lengthening the Nano Resonators for Tuning Down. Experimentally, four frequency tuning processes were conducted to demonstrate the possibility to tune down the resonant frequencies of nano resonators: (A) carbon-based nano resonator with added carbon deposition, (B) carbon-based nano resonator with added tungsten deposition, (C) tungsten-based nano resonator with added tungsten deposition, and (D) tungsten-based nano resonator with added carbon deposition. In all cases, nano resonators with similar lengths as well as the added lengths have been fabricated for better comparisons. Figure 4 shows the detailed experimental results

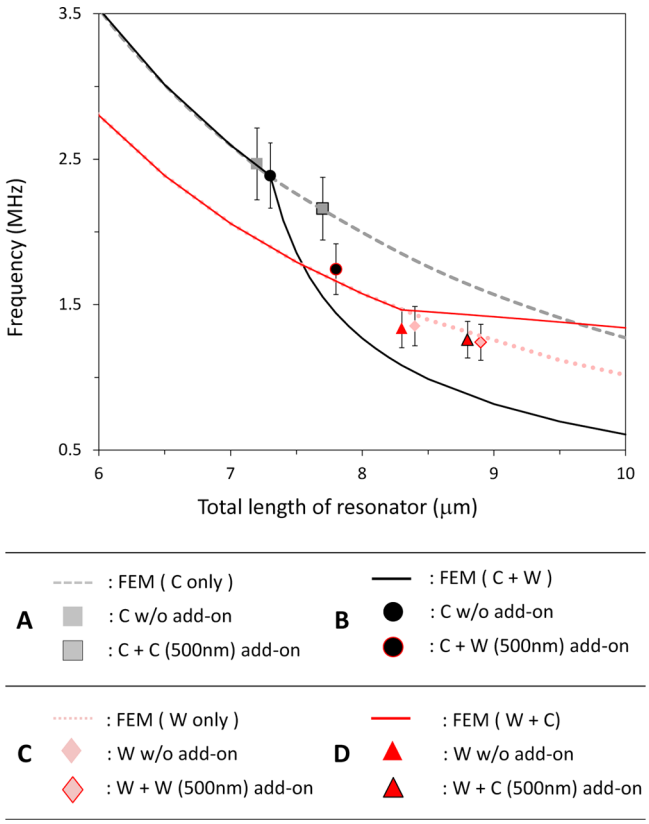

Figure 4. Frequency reductions of nano resonators by means of adding newly deposited length segments with nominal length of 500 nm at the end of the nano resonators. (A) Carbon segment added on carbon-based nano resonator. (B) Tungsten segment added on carbon-based nano resonator. (C) Tungsten segment added on tungsten-based nano resonator. (D) Carbon segment added on tungsten-based nano resonator. The FEM simulation results (solid and dotted lines) show good consistency with measurement data. Measurement error is estimated as ±5% originated from measurement uncertainty based on visual detections.

together with FEM simulation using ANSYS while Table 2 summarizes key results. Specifically, when a 500 nm-long carbon is added to a carbon-based nano resonator of 7.2 μm in length and 150 nm in diameter, resonant frequency is tuned from 2.467 to 2.159 MHz, resulting in a net 307.7 kHz frequency reduction as illustrated in group (A) in Figure 4. When a carbon-based nano resonator of 7.3 μm in length and 150 nm in diameter with resonant frequency at 2.386 MHz is added with 500 nm-long tungsten, its resonant frequency is reduced to 1.7436 MHz as shown in group B in Figure 4. The shorter length, carbon-based resonator showed higher resonant frequency than the tungsten-based one. When the length is increased, inversely and proportional as a factor of two, the gap decreases indicating that length is becoming the more dominant factor. However, the concentration of gallium components changes depending on the deposition parameters such as ion dose and irradiation dwell time, which then has an impact on both density and Young's modulus. Such variation in material property of deposits is one of the drawbacks, yet it implies versatile processing possibility as well. Similarly, the resonant frequency of a tungsten-based nano resonator with initial length of 8.3 μm and 150 nm diameter is measured at 1.352 MHz. When a 500 nm-long carbon material is added, the resonant frequency shifts down to 1.241 MHz which corresponds to a 111.2 kHz frequency reduction as illustrated in group D in Figure 4. In case of an 8.4 μm-long tungsten nano resonator, the extra added length of 500 nm tungsten decreases the resonant frequency from 1.337 to 1.259 MHz with a net frequency turning of 78.3 kHz as illustrated in group C in Figure 4. It can be inferred from the result that adding tungsten to carbon is much more effective in tuning down than adding carbon compared to vice versa. For the tungsten-based nano resonator, a smaller frequency reduction was observed by adding carbon material when compared with adding tungsten material of similar length.

3.2. Alternating Deposition Materials. In order to further illustrate the capability of the frequency tuning process, three successive material add-on processes of similar lengths of 500 nm-long carbon and tungsten were conducted on a tungsten nano resonator of 8.4 μm in length and 150 nm in diameter as depicted in Figure 5. The inset image shows the SIM image of the nano resonator with three successive tuning processes. Before and after each deposition step, the resonant frequency, the shift of resonant frequency, and the corresponding maximum lateral amplitude were recorded. After the three-step process, the total length was lengthened to 10.2 μm with a resonant frequency at 1.021 MHz. As demonstrated, alternating depositions as demonstrated should give another degree of freedom in controlling the frequency tuning process; however, multiple tests showed that more than four successive depositions were challenging to maintain the straight cylindrical shape of the nano resonators, which led to deviation in target tuning frequency.

3.3. Frequency Tuning UP via Coarse and Fine Trimming. The frequency tuning process to increase the resonant frequency was performed in both coarse and fine

Table 2. Frequency Tuning Down Process Result

resonator material	test number	original length (μm)	add-on (tuning) material/length (nm)	RF before tuning (MHz)	RF after tuning (MHz)	tuned range (kHz)
carbon based	1	7.2	carbon/≈500	2.467	2.1593	307.7 ↓
	2	7.3	tungsten/≈500	2.3858	1.7436	642.2 ↓
tungsten based	3	8.4	tungsten/≈500	1.352	1.2408	111.2 ↓
	4	8.3	carbon/≈500	1.3368	1.2585	78.3 ↓

dx.doi.org/10.1021/am402738g | ACS Appl. Mater. Interfaces 2013, 5, 9684−9690

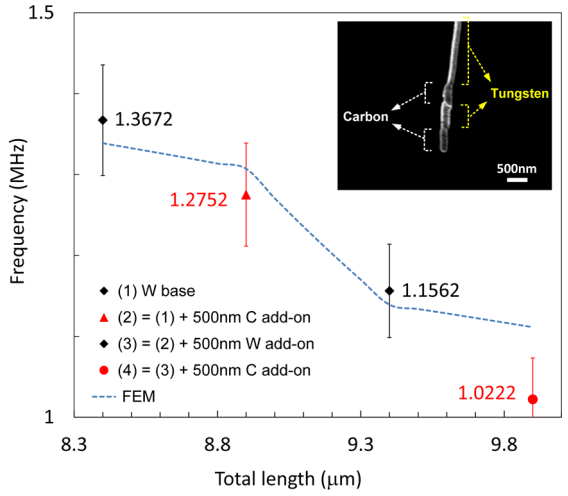

Figure 5. Frequency reductions of nano resonators via adding segments of different materials. Three 500 nm-long segments of either carbon or tungsten in alternating order have been sequentially deposited on a tungsten-based nano resonator. FEM simulation results are shown in blue dashed lines which follow the trend of experimental results except the third deposition (4). Deformation and slight thickening caused lower resonant frequency than simulation. (The unit for the numbers in the graph is MHz.)

manners as recorded in Figure 6. When a large amount of frequency adjustment is needed, direct cutting of a suitable portion of the cantilever-shape resonator at the tip region is a fast and effective way. After the coarse tuning step, fine tuning can be performed by exposing the nano resonator to continuous ion sputtering in the longitudinal direction in order to minimize the effective hitting area for better process

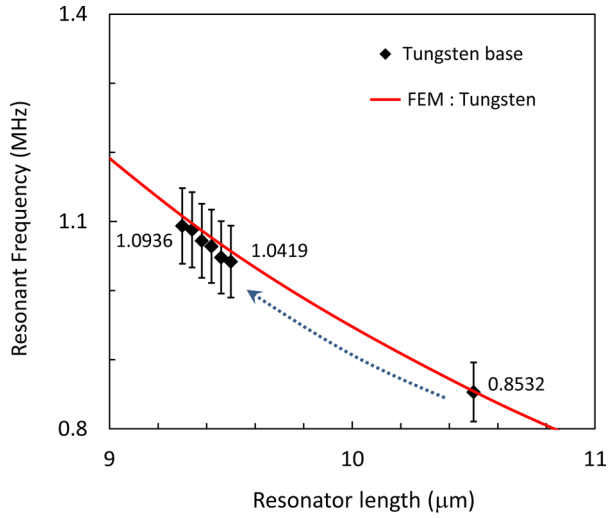

Figure 6. Coarse and fine cutting processes to increase the resonant frequency of a tungsten-based nano resonator. The coarse cutting process is conducted by applying the FIB sputtering beam perpendicular to the length of the nano resonator with a target length reduction of 1 μm. The fine and continuous cutting process is followed in the longitudinal direction to the length of the nano resonator at 300 pA of current. Six measurement points with 30 s of measurement interval have been recorded as shown. Within these 3 min, the ion beam irradiation removed about a total of a 200 nm-long segment. The experimental results are consistent with the FEM simulation predictions. (The unit for the numbers in the graph is MHz.)

control. It was found that the continuous fine-tuning process in the longitudinal direction of the nano resonator resulted in sharpened shape at the tip of the nano resonator (Figure 3d). Experimentally, a 1 μm-long segment was cut from a 10.5 μm-long tungsten nano resonator via the FIB sputtering process in the direction perpendicular to the nano resonator, leading to 188.7 kHz up-shift. The fine tuning process was conducted subsequently in the longitudinal direction of the nano resonator. The resonant frequency shift was monitored every 30 seconds under an ion beam of 300 pA as shown in Figure 6. Trimming was conducted until a 50 kHz up-shift, and about a 200 nm-long piece of tungsten ended up with the 51.7 kHz frequency increment.

Long-time exposure of the nano resonator to the high energy ion beam (30 kV) may affect the material properties such as density such that an undesired frequency shift may occur. Especially, the carbon-based nano resonator is easily influenced by the direct ion beam irradiation and requires more cautious manipulation during the process. We suspect that the relatively low Young's modulus and low density of carbon compared to that of tungsten make carbon-based resonators more sensitive to the ion beam sputtering process. Further, the FIB-CVD is a site specific method to produce nano/microstructures on the surface. As such, understanding the nature of the interface formed during FIB-CVD provides important information not only for design but also for the evaluation of the final product. In contrast to conventional CVD processes, FIB-CVD relies on relatively high local pressure ranging between 0.1 and 10 mTorr while the remaining chamber stays in the 10^{-6} Torr level. Such local pressure variation plays a key role in FIB-CVD while conventional CVD generally relies on a high temperature process. The introduced precursor gases are volatile while delivered near the target spot; however, the precursor density should be kept high enough to be absorbed in and build deposition upon beam irradiation. Not enough density or local pressure may cause weakness in deposited materials which later brings reliability issues of the device. To evaluate the strength of the interface between nano pillars and silicon substrate, extreme resonance was induced until the resonator failed. Figure 7 shows a 15 μm in length carbon-based nano resonator right before mechanical failure. It is noted that the failure occurred due to physical contact with the rotor and not from the interface between resonator and silicon substrate. No physical degradation was monitored in 30 minutes of operation as well. Reducing Ga^+ concentration in deposits is another issue to enhance the interface as up to 28 mol % of Ga^+ concentration was reported in FIB-CVD using a platinum precursor.[23] Having impurities such as carbon and gallium compounds in deposits is inevitable in FIB-CVD, yet lowering such concentrations is one of the major challenges in future FIB-CVD to extend potential applications.

4. CONCLUSION

In situ fabrication and passive frequency tuning of carbon- or tungsten-based cantilever-shape nano resonators and their frequency tuning of both directions of increasing and decreasing were successfully demonstrated. The FIB-CVD machining process was shown to be an effective way to build nano resonators as well as a useful tool to tune their resonant frequencies by either sputtering or deposition processes. The deposition process was used to add additional lengths on the nano resonators to reduce the resonant frequencies by 500 nm unit length, whereas the sputtering process was used to trim the

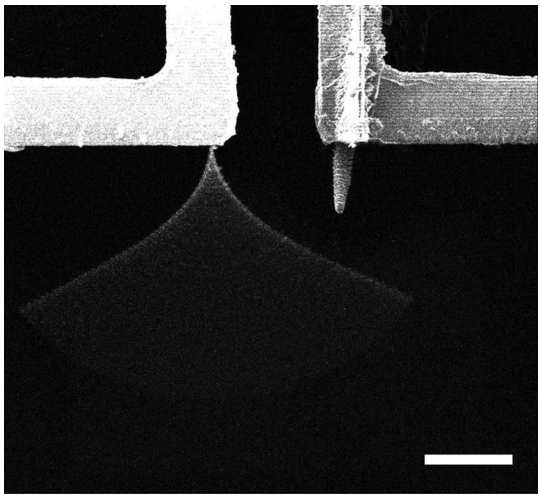

Figure 7. Extreme resonance of nano resonator. The nano resonator was forced to vibrate at higher excitation source input to test reliability of the interface between silicon substrate. Along with increasing input power, the resonator failed when it made contact with the rotor, suggesting that the root part was firmly fixed on the substrate. Scale bar: 5 μm.

nano resonators by cutting their lengths perpendicularly or longitudinally. No structural degradation was observed in either carbon- or tungsten-based nano resonators under 30 min of continuous excitation, and the experimental results matched well with numerical FEM predictions. The interface between a substrate and CVD deposits was tested via excessive resonance, and promising mechanical reliability was confirmed. As such, the developed tuning method could be applied to fabricate micro/nano resonators with efficient and bidirectional frequency tuning.

AUTHOR INFORMATION

Corresponding Author

*Tel: +82-2-2123-2812. E-mail: kimjb@yonsei.ac.kr.

Notes

The authors declare no competing financial interest.

ACKNOWLEDGMENTS

This research was supported by the Center for Integrated Smart Sensors as Global Frontier Project (CISS-2012M3A6A6054201), the Fusion Research Program for Green Technologies (NRF-2010-0019088) through the National Research Foundation of Korea funded by the Ministry of Science, ICT and Future Planning, and the National Research Foundation of Korea Grant (NRF-2012R1A1A2043661) funded by the Korean Government.

REFERENCES

(1) Wen, Y.; Ping, L.; Jin, Y.; Min, Z. *IEEE Sens. J.* **2004**, *4*, 828−836.
(2) Leland, R. P. *Proc. 40th IEEE Conf. Decis. Control* **2001**, *4*, 3447−3452.
(3) Kim, H. T.; Park, J.-H.; Kim, Y.-K.; Kwon, Y. *IEEE Microwave Wireless Compon. Lett.* **2002**, *12*, 432−434.
(4) Yao, J. J.; MacDonald, N. C. *J. Micromech. Microeng.* **1995**, *5*, 257−264.
(5) Scheibner, D.; Mehner, J.; Reuter, D.; Gessner, T.; Dotzel, W. *Proc. 16th Ann. Int. Conf. Micro Electro Mech. Syst.* **2003**, 526−529.
(6) Lee, K. B.; Lin, L.; Cho, Y.-H. *Proc. 17th IEEE Micro Electro Mech. Syst. Conf.* **2004**, 257−260.
(7) Syms, R. R. A. *J. Microelectromech. Syst.* **1998**, *7*, 164−171.
(8) Remtema, T.; Lin, L. *Sens. Actuators, A* **2001**, *91*, 326−332.
(9) Chiao, M.; Lin, L. *J. Micromech. Microeng.* **2004**, *14*, 1742−1747.
(10) Joachim, D.; Lin, L. *J. Microelectromech. Syst.* **2003**, *12*, 193−200.
(11) Enderling, S.; Brown, C. L.; Balakrishnan, M.; Hedley, J.; Stevenson, J. T. M.; Bond, S.; Dunare, C. C.; Harris, A. J.; Burdess, J. S.; Mitkova, M.; Kozicki, M. N.; Walton, A. J. *Proc. 18th IEEE Int. Conf. Micro Electro Mech. Syst.* **2005**, 159−162.
(12) Courcimault, C. G.; Allen, M. G. *Proc. 13th Int. Conf. Solid-State Sens., Actuators Microsyst.* **2005**, *1*, 875−878.
(13) Kim, K.; Jensen, K.; Zettl, A. *Nano Lett.* **2009**, *9*, 3209−3213.
(14) Kometani, R.; Funabiki, R.; Hoshino, T.; Kanda, K.; Haruyama, Y.; Kaito, T.; Fujita, J.; Ochiai, Y.; Matsui, S. *Microelectron. Eng.* **2006**, *83*, 1642−1645.
(15) Igaki, J.-y.; Kometani, R.; Nakamatsu, K.-i.; Kanda, K.; Haruyama, Y.; Ochiai, Y.; Fujita, J.-i.; Kaito, T.; Matsui, S. *Microelectron. Eng.* **2006**, *83*, 1221−1224.
(16) Syms, R. R. A.; Moore, D. F. *Electron. Lett.* **1999**, *35*, 1277−1278.
(17) Enderling, S.; Hedley, J.; Jiang, L.; Cheung, R.; Zorman, C.; Mehregany, M.; Walton, A. J. *J. Micromech. Microeng.* **2007**, *17*, 213−219.
(18) Igaki, J.-y.; Nakamatsu, K.-i.; Kometani, R.; Kanda, K.; Haruyama, Y.; Kaito, T.; Matsui, S. *J. Vac. Sci. Technol., B* **2006**, *24*, 2911−2914.
(19) Englander, O.; Christensen, D.; Kim, J.; Lin, L.; Morris, S. J. S. *Nano Lett.* **2005**, *5*, 705−708.
(20) Ishida, M.; Fujita, J.-i.; Ochiai, Y. *J. Vac. Sci. Technol., B* **2002**, *20*, 2784−2787.
(21) Ishida, M.; Fujita, J.; Ichihashi, T.; Ochiai, Y.; Kaito, T.; Matsui, S. *J. Vac. Sci. Technol., B* **2003**, *21*, 2728−2731.
(22) Chang, J.; Min, B.-K.; Kim, J.; Lee, S.-J.; Lin, L. *Smart Mater. Struct.* **2009**, *18*, 065017.
(23) Tao, T.; Ro, J.; Melngailis, J.; Xue, Z.; Kaesz, H. D. *J. Vac. Sci. Technol., B* **1990**, *8*, 1826−1829.
(24) Gere, J. M.; Timoshenko, S. P. *Mechanics of Materials*, 4th ed.; Pws Pub Co: Boston, 1997; Ch. 2.
(25) Kometani, R.; Nishi, S.; Warisawa, S.; Ishihara, S. *J. Vac. Sci. Technol., B* **2011**, *29*; DOI: 10.1116/1.3662493.